Proposed test of the time independence of the fundamental constants α and m_e/m_p using monolithic resonators

C. Braxmaier, O. Pradl, H. Müller, A. Peters, and J. Mlynek*
Fachbereich Physik, Universität Konstanz, D-78457 Konstanz, Germany

V. Loriette
ESPCI, Laboratoire d'Optique Physique, 10, rue Vauquelin 75231 Paris cedex 5, France

S. Schiller†
Institut für Experimentalphysik, Heinrich-Heine-Universität Düsseldorf, D-40225 Düsseldorf, Germany

A novel method is proposed for a laboratory test of the time independence of the fine-structure constant and of the electron to proton mass ratio, employing only electromagnetic resonators. For a resonator made out of a dielectric ionic or molecular crystal, the resonance frequencies depend on the product $\alpha^2 \sqrt{m_e/m_p}$ through the index of refraction. A test of the time independence of α and m_e/m_p can be performed by a search for a long-term change in the difference of two resonance frequencies exhibiting different dispersion. The method can be advantageously implemented with a single resonator. The prospects of implementation using optical resonators, systematic effects, and experimental requirements for a test at the level of 4×10^{-15}/yr relative variation in α or m_e/m_p are discussed. On the experimental side, birefringent monolithic sapphire optical resonators with high-reflectivity mirrors are fabricated and characterized. The measurements of optical materials with ultralow absorption loss (ppm/cm level), required for the proposed method, are also reported.

I. INTRODUCTION

The equivalence principle of general relativity postulates in its principle of local position invariance that the nongravitational fundamental constants of nature are independent of time [1]. In theories attempting a unification of gravity with the other fundamental forces, it is found that a violation of the equivalence principle may occur and that it can be consistently described. String theory, for example, predicts the existence of new fields, such as the dilaton field, which couples to matter. The particle masses and the fine-structure constant are functions of the dilaton field. If some masses move relative to an observation point—for example, due to the universe's expansion—the dilaton field value at the observation point could be time dependent, provided the coupling between hadrons and the dilaton field is nonzero. As a consequence, the fundamental constants may become time dependent. Another scenario is that of the existence of additional, compactified spatial dimensions. If the size of the compact dimensions is time varying, so are the coupling constants and masses [2].

With this theoretical motivation, there has recently been strong interest in performing observations constraining temporal variations of various fundamental constants. The basic principle is to compare the oscillation frequencies of two dissimilar systems ("clocks"), ω_1 and ω_2, over a sufficiently long time. The condition to be satisfied by the two systems defining these frequencies is

$$\frac{1}{\omega_1} \frac{\partial \omega_1}{\partial \beta} \neq \frac{1}{\omega_2} \frac{\partial \omega_2}{\partial \beta}, \tag{1}$$

where β is some fundamental (dimensionless) constant. This relation implies a different algebraic dependence of the frequencies on β. The dimensionless ratio of the frequencies is then a function of β, and the experiment seeks to measure how constant this ratio is over time.

Two approaches have been followed: astrophysical or geophysical observations and laboratory experiments. The first constrain the difference of the constant's values at times separated by a significant fraction of the age of the universe. Laboratory tests cover only a relatively short time span in the present. Their advantage, on the other hand, is their (relative) simplicity, reproducibility, and high precision. An overview of recent results is shown in Table I. As can be seen, the laboratory limits are weaker than the astrophysical limits, and therefore there is the need for a new generation of experiments. Moreover, the laboratory limit for m_e/m_p is significantly lower than that for α, so its improvement should be given particular attention.

The purpose of this paper is to propose a novel laboratory method to test the time independence of α and m_e/m_p, a method that is based on monolithic resonators, in particular on the use of a single resonator. The approach is conceptually simple, and unlike previous laboratory experiments, the two oscillator frequencies are obtained from two physically similar systems. The feasibility of achieving tests at the level of 4×10^{-15}/yr will be discussed. The basic physical effect that is used is the dependence of the index of refraction on α and m_e/m_p [12].

This paper is structured as follows. In Sec. II, we derive

*Present address: Humboldt-Universität zu Berlin, D-10099 Berlin, Germany.
†Email address: stephan.schiller@uni-duesseldorf.de

TABLE I. Selected tests of the time independence of fundamental constants. First section: geophysical and astrophysical tests. Second section: laboratory tests. X is the tested quantity. For astrophysical tests, the third column is $\Delta X/T$ where ΔX is the experimental limit.

System	X	Look-back time, redshift	Upper limit for $|\dot{X}/X|$	Ref.
Oklo natural reactor	α	1.8 Gyr	7×10^{-17}/yr	[3]
Fe II/Mg II	α	$z=0.8$	5×10^{-16}/yr	[4]
Si IV	α	$z=2.8-3.5$	4×10^{-14}/yr	[5]
Primordial nucleosynthesis	α	8.9 Gyr	1×10^{-14}/yr	[6]
H_2/H	$g_p\alpha$	$z=0.7$	4×10^{-15}/yr	[7]
H_2	m_e/m_p	$z=2.81$	9×10^{-14}/yr	[5]
H_2	m_e/m_p	$z=2.81$	1.5×10^{-14}/yr	[8]
H/C I	$g_p m_e/m_p\alpha^2$	$z=1.8$	4×10^{-15}/yr	[5]
Hg^+/H	α		4×10^{-14}/yr	[9]
Cs/Mg	$g_I m_e/m_p$		5×10^{-13}/yr	[10]
Cs/microwave cavity	$g_I m_e/m_p\alpha^3$		4×10^{-12}/yr	[11]

the dependence of the refractive index of certain media on α and m_e/m_p. In Sec. III we consider monolithic optical resonators and present a calculation of how the resonance frequencies are affected by changes in the fundamental constants α and m_e/m_p. Section IV discusses systematic effects and gives feasibility estimates for a test with a significantly higher sensitivity than present laboratory tests. Experimental work that aims at achieving this goal is described in Sec. V. Appendixes discuss a method for increasing the sensitivity of the proposed scheme and a magneto-optical systematic effect.

II. DEPENDENCE OF THE REFRACTIVE INDEX ON α AND m_e/m_p

We consider an electromagnetic resonator filled with a dielectric medium of refractive index n. The dependence of $n(\alpha,m_e/m_p,\omega)$ on the fundamental constants α, m_e/m_p, and frequency ω of the wave circulating in the resonator is of central interest and will be analyzed in the following. We use SI units throughout, so that $\alpha=e^2/4\pi\epsilon_0\hbar c$.

In the local field model [13], the refractive index is related to the susceptibility χ by

$$\frac{n(\omega)^2-1}{n(\omega)^2+2}=\frac{\chi(\omega)}{3}. \qquad (2)$$

We shall assume an ionic crystal, where the dielectric susceptibility is due to both electrons and optical phonons. Examples for such crystals are Al_2O_3 (sapphire), CaF_2, KCl, etc. In the transparency range, i.e., when the frequency ω significantly exceeds the largest optical phonon frequency, the multiphonon absorption can be extremely low [14,15,41]. In this range the susceptibility has the following approximate dispersion relation:

$$\chi(\omega)=\chi_{at}+\frac{e^2}{\epsilon_0}\sum_i\frac{N_i}{M_i}\frac{f_i}{\Omega_i^2-\omega^2}, \qquad (3)$$

where χ_{at} is the susceptibility due to the electrons, M_i is the reduced effective mass of the ith optical mode, N_i is the effective number density of the ion group involved in mode i, and f_i are oscillator strengths [17]. The optical phonon frequencies Ω_i may be written as

$$\Omega_i=\hat{\Omega}_i\sqrt{\frac{m_e}{M_i}}\frac{E_R}{\hbar}, \qquad (4)$$

where $E_R=\alpha^2 m_e c^2/2$ is the Rydberg energy, and $\hat{\Omega}_i$ is a dimensionless constant of order unity with corrections of order α and m_e/m_p and higher. This scaling arises from the scales involved in the interatomic potential $V(R)$. Since the potential depth and extension are on the order of E_R and a_0, respectively, the curvature of the potential at the minimum is $d^2V/dR^2\sim E_R/a_0^2$. From $d^2V/dR^2\sim M_i\Omega_i^2$ follows Eq. (4).

We assume now that the ratios of nuclear masses are constant in time [18]. We may then write the effective mass M_i of an optical mode as m_p times a mode-dependent, but time-independent, constant $\hat{m}_i$. Thus, the dependence of the phonon frequencies on the fundamental constants is given by

$$\Omega_i=\bar{\omega}_i\sqrt{\frac{m_e}{m_p}}\alpha^2, \quad \bar{\omega}_i=\pi\frac{\hat{\Omega}_i}{\sqrt{\hat{m}_i}}\frac{c}{\Lambda}, \qquad (5)$$

where $\Lambda=h/m_e c$ is the electron's Compton wavelength and c/Λ may be regarded as a fundamental frequency scale. We do not need to consider the possibility of a temporal change in this scale, which is *not* a dimensionless quantity, since such a change could not be observed by any experiment that is based on this scale. Indeed, by explicit inclusion of c/Λ as a variable quantity in the following calculation it is found to drop out in the final result, Eq. (16). The reduced mode frequencies $\bar{\omega}_i$ can thus be regarded as constants.

Turning to the other quantities in the susceptibility, we note that the oscillator strength f_i is of order unity for an allowed transition and approximately independent of the fundamental constants. Concerning the number density N_i, we

recall that the characteristic interparticle distance in the medium is of order of the Bohr radius a_0. Thus,

$$N_i \sim a_0^{-3} = \left(\frac{\alpha m_e c}{\hbar} \right)^3. \tag{6}$$

For simplicity, we neglect for the moment the frequency dependence of the atomic susceptibility χ_{at} for the range of frequencies considered here. Inclusion is easily possible and is treated below in Sec. III B. Then χ_{at} may also be taken as a constant of order unity and is also independent of the fundamental constants to lowest order.

Combining Eqs. (2)–(6), we find

$$\frac{n(\alpha,m_e/m_p,\omega)^2-1}{n(\alpha,m_e/m_p,\omega)^2+2} = \frac{\chi_{at}}{3} + \sum_i \frac{F_i}{1-(m_p/m_e)\alpha^{-4}\omega^2/\bar{\omega}_i^2}, \tag{7}$$

where the F_i are dimensionless factors independent of α and m_e/m_p. Thus, the dependence of the refractive index on these two constants comes only from the dependence of the phonon frequencies on them.

By calculating the total derivative of the left hand sides in Eq. (7) with respect to α, m_e/m_p, and ω, it is easy to verify that

$$\alpha \frac{\partial n(\alpha,m_e/m_p,\omega)}{\partial \alpha} = -2\omega \frac{\partial n(\alpha,m_e/m_p,\omega)}{\partial \omega}, \tag{8}$$

$$\frac{m_e}{m_p} \frac{\partial n(\alpha,m_e/m_p,\omega)}{\partial m_e/m_p} = -\frac{\omega}{2} \frac{\partial n(\alpha,m/m_p,\omega)}{\partial \omega}. \tag{9}$$

These relations are useful, since they permit one to determine the ''sensitivity'' of a medium's refractive index to α and m_e/m_p experimentally by a standard measurement of the dispersion, rather than requiring a theoretical calculation of the solid-state properties.

III. CONCEPT OF THE MEASUREMENT

From the above it is clear that any measurement sensitive to a variation of the index of refraction of a medium is sensitive to a variation of α and m_e/m_p. The most sensitive measurement of variations in n is the measurement of variations of the resonance frequency of an electromagnetic cavity filled with the medium, provided the dimensions of the cavity are kept sufficiently stable. In order to avoid density fluctuations associated with a gaseous filling medium, we are led to consider solid (monolithic) resonators, in which the electromagnetic wave is fully confined in the solid. For simplicity, we shall assume a monolithic resonator with a homogeneous refractive index. Such monolithic resonators have been developed both for microwave frequencies (whispering gallery resonators, notably made from sapphire) and for optical frequencies (whispering gallery resonators and Gaussian mode resonators) [27].

Consider a monolithic resonator to which an oscillator is frequency locked. Under lock, the oscillator's frequency ω is given by

$$n(\omega)(\omega-\omega_e)L_{rt} = 2\pi qc. \tag{10}$$

Here L_{rt} is the round-trip path length for the resonating wave, and q is an integer. ω_e describes the detuning of the oscillator frequency from the exact resonance due to lock errors, with $|\omega_e| \ll \omega$. The contribution of the mirror reflection phase shifts on the dependence of ω on the fundamental constants can be neglected if they exhibit small dispersion. We shall interpret ω, L_{rt}, and n as being average values for a certain measurement time.

The oscillator frequency ω will depend on α and m_e/m_p via n. However, the resonator length L_{rt} is also a function of α. Moreover, there are external influences which can affect n, ω_e, and L_{rt}: both the length and the index are also functions of the resonator temperature, and may be time varying due to microscopic changes in the structure of the medium (creep). The lock error ω_e depends on noise levels and offsets in the electronics, and on the beam coupling geometry, and may also drift in time. We therefore introduce the variations Δn, $\Delta \omega$, $\Delta \omega_e$, ΔL_{rt}, which under conditions of lock are related by

$$\frac{\Delta n}{n} + \frac{\Delta \omega - \Delta \omega_e}{\omega} + \frac{\Delta L_{rt}}{L_{rt}} = 0, \tag{11}$$

and ω_e was neglected in the second denominator. We must now take into account that the index change Δn must include the change in the oscillator's frequency:

$$\Delta n = \Delta \omega \frac{\partial n}{\partial \omega} + \Delta \alpha \frac{\partial n}{\partial \alpha} + \Delta \left(\frac{m_e}{m_p} \right) \frac{\partial n}{\partial m_e/m_p} + \Delta n|_e. \tag{12}$$

The last term summarizes extrinsic variations due to temperature variations, etc.

The resonator length has an intrinsic dependence on α since $L_{rt} \sim a_0 = \Lambda/\alpha$. Therefore,

$$\Delta L_{rt} = \frac{\partial L_{rt}}{\partial \alpha} \Delta \alpha + \Delta L_{rt}\Big|_e = -L_{rt} \frac{\Delta \alpha}{\alpha} + \Delta L_{rt}\Big|_e. \tag{13}$$

Here $\Delta L_{rt}|_e$ are extrinsic variations due to temperature changes, etc. Combining the last four expressions, we arrive at

$$\frac{\Delta \omega}{\omega} = \frac{2\bar{n}+1}{\bar{n}+1} \frac{\Delta \alpha}{\alpha} + \frac{\bar{n}/2}{\bar{n}+1} \frac{\Delta(m_e/m_p)}{m_e/m_p}$$
$$-\frac{1}{\bar{n}+1} \left(\frac{\Delta L_{rt}|_e}{L_{rt}} + \frac{\Delta n|_e}{n} - \frac{\Delta \omega_e}{\omega} \right). \tag{14}$$

We have introduced the normalized dispersion $\bar{n}(\omega) = n^{-1}\omega\partial n(\omega)/\partial\omega$.

This expression shows how it is possible to perform a test of the time independence of α or m_e/m_p: one compares two oscillators, one of which (say, ω_1) is locked to a monolithic resonator. To be sensitive to a variation of alpha, the second oscillator must then satisfy the condition [see Eq. (1)]
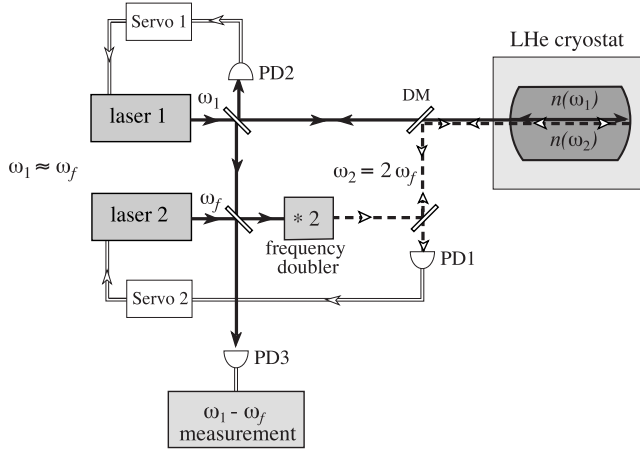
FIG. 1. Schematic of the apparatus for the proposed test. Two laser frequencies ω_1 and $\omega_2 = 2\omega_f$ are stabilized to modes of a monolithic resonator operated in an ultrastable environment. Variations in the fundamental constants α and m_e/m_p change the refractive indices $n(\omega_1)$, $n(\omega_2)$ by different amounts so that a change in the laser frequency difference $\omega_1 - \omega_f$ occurs. DM: dichroic mirror. PD1 and PD2: error signal photodetectors. PD3: beat frequency photodetector.

$$\frac{\alpha}{\omega_2}\frac{\partial \omega_2}{\partial \alpha} \neq \frac{2\bar{n}_1 + 1}{\bar{n}_1 + 1}, \tag{15}$$

or analogously for m_e/m_p. However, the second oscillator must not necessarily be of a different nature from the first, such as an atomic clock. It is possible to compare two oscillators locked to two or even a *single* resonator. This is a significant advantage, since only one type of experimental know-how is then required. In the two-resonator implementation, the second resonator may be a "vacuum"-type (i.e., nonmonolithic) resonator, as is commonly used for laser frequency stabilization, in which case $\bar{n}_2 = 0$. For the single-resonator approach, the resonator must be configured such that two independent waves resonate in it that satisfy $\bar{n}_1 \neq \bar{n}_2$. This can be achieved by using (i) An isotropic medium and two waves of widely different frequency, making use of the dispersion of $\bar{n}$, i.e., the second-order dispersion of the index, or (ii) an anisotropic (birefringent) medium and two waves of similar frequency, making use of the different dispersion of the ordinary (n_o) and extraordinary indices (n_{eo}).

A configuration in which the two waves can propagate along the same path (identical L_{rt}) can easily be implemented in both cases, simplifying the resonator further and giving a certain amount of common mode reduction of the extrinsic length change influence.

Figure 1 shows a schematic of a setup for a single-resonator experiment in the optical domain. Two similar lasers of emitting waves at frequencies ω_1 and ω_f are used. The monolithic resonator is interrogated by ω_1 and by the second harmonic of ω_f, which is generated in a nonlinear crystal. The resonator mirrors must have high reflectivity at both these frequencies. The two lasers are locked to respective modes of the monolithic resonator, making use of the

respective waves reflected from the resonator. The modes to which the lasers are locked are chosen such that the difference $|\omega_f - \omega_1|$ lies in the microwave or radio-frequency domain and can easily be measured. Its temporal stability is the quantity of interest.

We now calculate the sensitivity of this approach. We take $\omega_2 = p\omega_f$, where p is an integer, with the value of 2 being most relevant in practice (second harmonic), and $\omega_f \simeq \omega_1$. We obtain

$$\Delta\omega_f - \Delta\omega_1 = A\left(\frac{\Delta\alpha}{\alpha} - \frac{1}{2}\frac{\Delta(m_e/m_p)}{m_e/m_p} + \frac{\Delta L_{rt}|_e}{L_{rt}}\right) + \frac{\omega_1}{1 + \bar{n}_1}$$

$$\times \frac{\Delta n_1|_e}{n_1} - \frac{\omega_1}{1 + \bar{n}_2}\frac{\Delta n_2|_e}{n_2} + \frac{\Delta\omega_{e2}/2}{1 + \bar{n}_2} - \frac{\Delta\omega_{e1}}{1 + \bar{n}_1}. \tag{16}$$

The material constant A is

$$A = \omega_1(\bar{n}_2 - \bar{n}_1)/(1 + \bar{n}_1)(1 + \bar{n}_2), \tag{17}$$

and the relevant indices are $n_1 = n_{eo,o}(\omega_1)$, $n_2 = n_{eo,o}(\omega_2)$. Note that the opposite signs of the prefactors of $\Delta\alpha$ and $\Delta(m_e/m_p)$ come from the fact that the resonator length depends on α but not on m_e/m_p.

A first important result is that the effect of a path length change $\Delta L_{rt}|_e$ is as large as that of a change in α. To discuss Eq. (16) further, we distinguish two cases. The case of strong dispersion, achievable through doping, is treated in Appendix A.

In standard materials the case of weak dispersion, $\bar{n}_i \ll 1$, applies. Equation (16) then reduces to

$$\Delta\omega_f - \Delta\omega_1 \simeq (\bar{n}_2 - \bar{n}_1)\omega_1\left(\frac{\Delta\alpha}{\alpha} - \frac{1}{2}\frac{\Delta(m_e/m_p)}{m_e/m_p} + \frac{\Delta L_{rt}|_e}{L_{rt}}\right)$$

$$+ \omega_1\left(\frac{\Delta n_1|_e}{n_1} - \frac{\Delta n_2|_e}{n_2}\right) + \frac{\Delta\omega_{e2}}{2} - \Delta\omega_{e1}. \tag{18}$$

Since the first term sought is multiplied by the small quantity $\bar{n}_2 - \bar{n}_1 \ll 1$, the influence of extrinsic changes on the indices and on the lock errors is relatively important. The next section discusses quantitatively their influence.

IV. SYSTEMATIC EFFECTS AND FEASIBILITY ESTIMATES

In this section we consider the systematic effects $\Delta L_{rt}|_e, \Delta n_i|_e, \Delta\omega_{ei}$, which will limit the resolution of an experiment searching for $d\alpha/dt$ or $d(m_e/m_p)/dt$. We also deduce experimental requirements for an experiment that seeks to improve the current *laboratory* limits on $|\alpha^{-1}d\alpha/dt|$ by an order of magnitude to 4×10^{-15}/yr and on $|m_p/m_e d(m_e/m_p)/dt|$ by a factor of 60 to 8×10^{-15}/yr (assuming no cancellation). The measurement time is 1 yr, a realistic value in view of past experience with optical resonators.

TABLE II. Dispersion difference $|\bar{n}(\lambda_2)-\bar{n}(\lambda_1)|/[1+\bar{n}(\lambda_1)][1+\bar{n}(\lambda_2)]=|A|/\omega_f=\bar{A}^{\lambda_1,\lambda_2}$ for several optical materials. The wavelengths are $\lambda_1=\lambda_f=1064$ nm and $\lambda_2=532$ nm. The subscripts refer to the polarizations of waves 1 and 2. o and eo denote the ordinary and extraordinary polarizations, respectively. Vitreous fused silica (v-SiO$_2$) and CaF$_2$ are optically isotropic media.

Material	$\bar{A}^{\lambda_1,\lambda_2}_{o,o}$	$\bar{A}^{\lambda_1,\lambda_2}_{eo,eo}$	$\bar{A}^{\lambda_1,\lambda_2}_{o,eo}$	$\bar{A}^{\lambda_1,\lambda_2}_{eo,o}$	$\bar{A}^{\lambda_1,\lambda_1}_{o,eo}$	$\bar{A}^{\lambda_2,\lambda_2}_{o,eo}$	Ref.
CaF$_2$	0.0071						[19,20]
MgF$_2$	0.0048	0.0048	0.0051	0.0045	0.00023	0.00032	[19,21]
Al$_2$O$_3$	0.014	0.013	0.013	0.013	0.004	0.0045	[22]
SiO$_2$	0.010	0.010	0.011	0.0097	0.000033	0.00010	[19,23]
v-SiO$_2$	0.0079						[24]

Materials that have been shown to exhibit low loss in the optical domain (see [15,41,16] and Sec. V) all fall in the class of weak dispersion. For a few materials, Table II gives the parameter A for different combinations of interrogating waves. We see that the use of two widely different frequencies gives A values that are more than an order of magnitude larger than if one uses the different dispersion of the ordinary and extraordinary polarizations in a birefringent medium at the same frequency. In the following we assume the value $|A|/\omega_1=0.01$ and a laser wavelength $2\pi c/\omega_1=1$ μm. Equation (18) implies that (i) the relative length change must be $|\Delta L_{rt}|_e/L_{rt}|<1\times10^{-15}$, (ii) the relative index changes must be $|\Delta n_i|_e/n_i|<1\times10^{-17}$, assuming the worst case where $\Delta n_1|_e$ and $\Delta n_2|_e$ are uncorrelated, and (iii) the lock error drift for either laser must be $|\Delta\omega_{ei}|/2\pi<3$ mHz.

Requirements (i) and (ii) indicate that a cryogenic resonator is the only option. Only in such resonators can the temperature dependence of the optical path lengths n_iL_{rt} and the aging (dimensional relaxation) be sufficiently low. The reasons for this are, respectively, that the thermooptic coefficient $\eta=n^{-1}dn/dT$ and the thermal expansion coefficient $\gamma=L_{rt}^{-1}dL_{rt}/dT$ decrease as T^3 at cryogenic temperature, and that there is little thermal energy available for activation of disclocation motion.

Requirements (i)–(iii) are discussed in turn below.

A. Dimensional stability

The thermal expansion coefficient of sapphire is $\gamma(2$ K$)=5\times10^{-12}$/K and would imply $|\Delta T|<0.2$ mK. However, the temperature stability required by condition (ii) is more stringent (see below).

Dimensional aging effects of a vacuum (i.e., nonmonolithic) sapphire cryogenic optical resonator have been studied over a long time (6 months). An upper limit (determined by the sensitivity of the measurement system) is $|\Delta L_{rt}|_e/L_{rt}|<2\times10^{-11}$ [25]. Experiments in our group are under development to increase the sensitivity and provide a tighter limit.

The gravitational force acting on the resonator slightly deforms it, changing in particular L_{rt}. If the orientation changes with respect to gravity, a change ΔL_{rt} will occur. Calculations show that at an offset tilt of 1 mrad, $\Delta L_{rt}/L_{rt}\simeq10^{-15}$ per mrad tilt change. Active tilt stabilization can be used to keep ΔL_{rt} within the required bounds.

B. Index of refraction stability

For sapphire, the thermo-optic coefficient is estimated to be $\eta=1\times10^{-11}$/K at 2 K. This leads to a temperature stability requirement $|\Delta T|<|\Delta n_i|_e/n_i|/\eta=1$ μK to satisfy requirement (ii). Such a temperature stability can be achieved over long time by active control. Note that a significant reduction of the temperature stability requirement could be obtained, if necessary, by working at sub-kelvin temperatures [26]. Also, the temperature dependences of n_1 and n_2 may turn out to be similar, which would reduce the temperature stability requirement.

The laser wave circulating in the resonator is to a significant fraction dissipated in it. The heating results in a change of the optical path length. The active temperature control of the resonator cannot fully regulate away the effects of a change in temperature along the light path, since the temperature sensor will be located at the boundary of the resonator. An estimate for a 10-cm-long sapphire resonator at cryogenic temperature is $\Delta n/n\simeq10^{-16}$ per μW change in dissipated power. This implies that the circulating power must be stable within 0.1 μW by controlling the input power. Since typical input powers are low, a few μW, this requirement is not difficult to meet.

The influence of external magnetic and electric fields on the index of refraction is treated in Appendix A. It can be kept sufficiently low by an appropriate choice of material and/or shielding.

The influence of aging on the index of refraction at cryogenic temperature is unknown.

C. Laser frequency lock stability

A lock error can arise for several reasons: drifts in electronic components in the servo system, spurious interference effects in the light path of the laser beam between resonator and photodetector, and changes in alignment of the wave entering into the resonator causing a change in coupling to higher-order resonator modes. The beam geometry must therefore be kept very stable over time. The lock error is proportional to the resonator linewidth, $|\Delta\omega_e|\simeq\delta\omega_r$, with the numerical factor $\delta\ll1$ being a function of averaging time.

For a level $\delta=1\times10^{-6}$ *over the assumed integration time of 1 yr*, a cavity linewidth on the order of $\omega_r/2\pi=3$ kHz is required to satisfy condition (iii). This imples a very
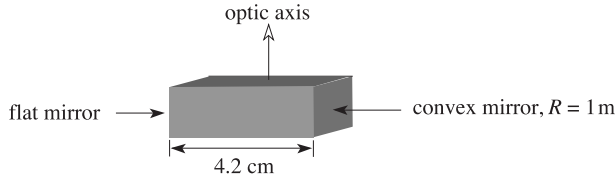
FIG. 2. Schematic of the monolithic sapphire resonator.

low bulk loss (scattering plus absorption) in the resonator, below $n\omega_r/c = 1$ ppm/cm.

We have recently studied lock errors for Nd:YAG lasers (with $\omega/2\pi = 280$ THz) locked to a cryogenic optical cavity (linewidth $\omega_r/2\pi = 50$ kHz) over medium time scales. On a time scale of 1 day lock error drifts at the level of 2 Hz/day were achieved [43]. This implies a relative lock accuracy of $\delta = 4 \times 10^{-5}$ over 1 day. Thus, satisfying the above requirement will require a very significant improvement in the ability to reduce lock error drifts.

V. EXPERIMENTAL RESULTS

In this section we describe the characterization of sapphire monolithic optical resonators [27].

Motivated by the absence of long-term dimensional drift of sapphire crystalline vacuum resonators [25] and the report of sapphire of low optical loss [16], we chose to develop sapphire monolithic resonators. Figure 2 shows a schematic of the sapphire monolithic resonators. Sapphire is a uniaxial crystal ($n_a = n_b \neq n_c$). The resonator was fabricated such that the crystal symmetry axis (c axis, optic axis) lies perpendicular to the resonator axis. The eigenpolarizations are therefore linearly polarized, parallel to the crystal axis with extraordinary index $n_{eo} = n_c = 1.7469$ at 1064 nm, and perpendicular to it with ordinary index $n_o = n_a = 1.7546$. The modes are split in frequency due to the birefringence (see the first case in Appendix A).

The plane and convex end faces of the standing-wave resonator were coated with high-reflection (HR) coatings for the center wavelength 1064 nm. A low transmission was specified since low bulk losses in the crystal were expected. The 8.4-cm round-trip path length implies a free spectral range of 2.0 GHz. The large radius of curvature (1 m) of the convex face leads to a nearly collimated resonator mode, with 200 μm waist. The base material was a nominally high-purity sapphire single-crystal rod (HEMEX ULTRA, Crystal Systems, Salem, MA). Two identical resonators were polished and coated by Research Electro-Optics (Boulder, CO).

The procedure employed to characterize the resonators was as follows. A 1064-nm monolithic diode-pumped Nd:YAG laser with single-frequency output (10 kHz linewidth) was mode matched to the TEM_{00} resonator mode, with typically 80% efficiency. The optical powers incident on, reflected from, and transmitted through the resonator on resonance were measured, as well as the mode-match efficiency to the TEM_{00} mode and the resonator linewidth. To determine the linewidths, frequency modulation sidebands were imparted to the laser wave at a known frequency so that a frequency calibration was possible. Figure 3 shows a reso-
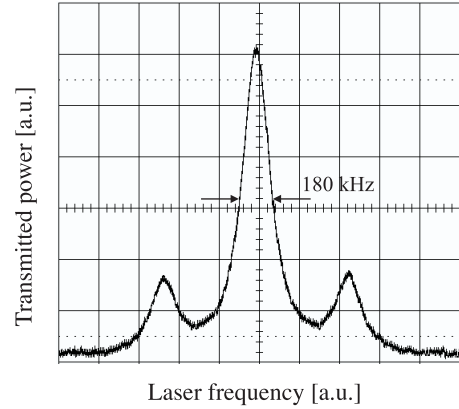

FIG. 3. Resonance line of a monolithic sapphire resonator. Transmitted power as a function of laser frequency is shown. The laser is phase modulated at 492 kHz, leading to satellite transmission peaks. The wavelength is 1064 nm.

nance of one of the two resonators, measured in transmission. Full width at half maximum (FWHM) linewidths of 180 kHz and 200 kHz were found for the two resonators. Finesses of 10 000 and overall losses of 600 ppm correspond to these values. No significant difference in linewidths was observed for the two orthogonal input polarizations.

From the measured quantities, the transmissions of both mirrors and remaining round-trip losses are found by invoking the standard Fabry-Perot formulas. Table III summarizes the characterization results. The derived mirror transmission values show that these have excellent reflectivity. The round-trip losses are the limiting factor for the linewidth of these resonators. Since these turned out to be significantly higher than expected, the low mirror transmission led to a very low in-coupling efficiency. To aid in understanding the origin of the losses, three further measurements were performed.

One of the resonators was cooled to 90 K, to test whether the internal loss exhibited a temperature dependence. No change in the linewidth was found within experimental accuracy.

The absorption loss of the bulk material at 1064 nm was measured on one of the resonators using the mirage method [32], with the beams aligned transversely to the resonator axis (the side faces were polished for that purpose). Values in the range $(9-12)\pm 3$ ppm/cm were found, implying that

TABLE III. Properties of two monolithic sapphire resonators at 1064 nm. The linewidths were measured; the other properties were calculated from measured couplings, transmissions, and mode-matching efficiencies.

Property	Resonator A	Resonator B
Linewidth	180 kHz	200 kHz
Total loss per round trip	550 ppm	630 ppm
Transmission T_1 of mirror 1	0.6 ppm	0.63 ppm
Transmission T_2 of mirror 2	2.5 ppm	2.2 ppm
Coupling efficiency from side 1	4×10^{-3}	4×10^{-3}
Coupling efficiency from side 2	18×10^{-3}	14×10^{-3}

TABLE IV. Absorption values of low-loss crystals, at a wavelength of 1064 nm, measured with the mirage method. Path length is the distance traversed by the absorbed laser beam. The absorption coefficient ξ is the average over this distance. Ranges imply that the absorption is not homogeneous in the direction perpendicular to the path length.

Material	ξ [ppm/cm]	Path length [mm]	Producer/supplier
CaF_2	2.5–2.8	38	Nishon
CaF_2	7.9–8.8	38	Schott
CaF_2	5.6–6.0	38	Schott
CaF_2	1.33±0.8	20	Korth
MgF_2	14.5–16.7	22	Nishon
SiO_2 (artificial quartz)	3.4±1	5	Steeg & Reuter
SiO_2 (natural quartz)	79±20	5	Steeg & Reuter
SiO_2 (natural quartz)	19±5	5	Steeg & Reuter
Al_2O_3 (sapphire)	9-12	10	Crystal Systems

the resonators have on the order of 100 ppm bulk absorption loss over the round trip.

To look for scattering losses, a high-power cw 532-nm laser beam was passed through the crystal. Scattered light could be observed. Without a quantitative measurement of the scattering it is, however, not possible to estimate its importance. In addition, orange fluorescence was observed. This indicates absorption by impurities, which are likely to be Cr^{3+} ions [33]. These ions should, however, only have minimal absorption at 1064 nm. The origin of the $\sim$500 ppm discrepancy between absorption loss and total loss per round trip thus remains largely unresolved. It could be scatter at the mirror-bulk interface, or absorption in the mirror, or bulk scatter plus fluorescence loss.

A reliable source for sapphire with losses at the few ppm/cm level is not known to the authors at present. Material of such quality is feasible but requires very pure starting compounds and growth methods that avoid contamination [34]. Perhaps the development of next-generation optical interferometers for gravitational wave detection will provide sufficient impetus for further development in this direction.

It is therefore important to study other crystalline materials as possible alternatives. We have performed measurements on quartz and calcium fluoride samples from different sources. Table IV summarizes the results. The lowest values around 2 ppm/cm (at 1064 nm) are among the lowest ever measured for crystals. The only material that shows similarly low loss is synthetic fused silica (a glassy material), as used in telecommunication fibers [27]. These values satisfy the level required for the proposed experiment (Secs. IV C and Appendix B).

VI. SUMMARY AND OUTLOOK

A conceptually simple method for a laboratory test of the constancy of α and m_e/m_p has been proposed. It is based on a monolithic resonator fabricated from a sufficiently strongly dispersive medium that also must possess very low loss. Two oscillators of sufficiently large frequency difference are frequency locked to the resonator and the temporal stability of the frequency difference between appropriate subharmonics is measured. While this method can be implemented in the

optical or in the microwave regime, in this paper we have focused our attention on the optical domain.

Requirements were derived for performing a significantly improved laboratory test of the time independence of α and m_e/m_p at the level of 4×10^{-15}/yr. The most stringent requirements to the resonator itself are very low aging effects and very low resonator loss. In addition, the electronic and optical system must provide a lock stability at the level of 1 ppm of resonator linewidth. We have proposed doping of the resonator material with a narrow-linewidth electronic or molecular species and shown that in such a case most stability requirements can be significantly relaxed.

In our experimental work two monolithic standing-wave sapphire resonators were fabricated and characterized. The result was the proof of principle that monolithic resonators with mirrors of near-unity reflectivity can be achieved. The bulk loss of the resonators was a factor of 10 higher than the required value. Therefore alternative materials were investigated with respect to absorption losses, and materials with the required loss level on the order of a ppm/cm were demonstrated (crystalline quartz and calcium fluoride). These are promising for achieving the discussed sensitivity goal. The planned work is to (i) develop monolithic resonators from ultralow-loss materials and appropriate high-reflectivity and low-internal-loss dielectric coatings that withstand cooling to cryogenic temperature, (ii) characterize and improve the laser lock instability over long time scales, (iii) perform a search for aging effects of the index of refraction at cryogenic temperature using a monolithic resonator, and (iv) perform a higher sensitivity search for aging effects of the resonator length.

Fused silica monolithic resonators should be included in the tests since the bulk loss in SiO_2 is ultralow [27] and dielectric coatings of similar low loss (finesse 200 000) that withstand cooling have already been demonstrated on fused silica substrates (using a vacuum resonator [31,35]). The fact that the thermal expansion coefficients of the above materials with demonstrated ultralow loss are significantly higher than that of sapphire [36] will need to be addressed. CaF_2 and fused silica are isotropic materials and so will require careful magnetic shielding. Furthermore, quartz is an optically active

material, although this property should not influence the resonance frequencies.

Studies (ii) and (iii) will benefit from use of the recently developed frequency comb method [37], which will allow a direct and accurate measurement of the frequency of a laser locked to an optical cavity.

ACKNOWLEDGMENTS

APPENDIX A: SENSITIVITY TO EXTERNAL FIELDS

External dc or low-frequency stray fields can change the index of refraction of a medium due to nonlinear-optical interaction. A clear example is electro-optic media. Their electro-optic coefficients have a sufficient magnitude that such media are unsuitable for the present purpose. Another example are magneto-optical effects, such as the Faraday effect. It is present in all media, also in inversion-symmetric ones, and will therefore be considered in some detail here.

For a given anisotropic medium and a given direction of light propagation, consider the coordinate system (x,y,z) spanned by the direction of propagation, z, and the directions x,y of the two orthogonal linear eigenpolarizations (in absence of magnetic field), as in Fig. 4. The dielectric tensor ϵ is Hermitian and takes the form

$$\epsilon = \begin{pmatrix} n_x^2 & -i\gamma B_z & i\gamma B_y \\ i\gamma B_z & n_y^2 & -i\gamma B_x \\ -i\gamma B_y & i\gamma B_x & n_z^2 \end{pmatrix}, \qquad \text{(A1)}$$

where n_x, n_y, n_z are the eigenindices in the absence of a magnetic field, γ is the magnetogyration coefficient, and (B_x, B_y, B_z) are the magnetic field coordinates in the chosen coordinate system [38]. The inverse square eigenindices and corresponding eigenpolarizations in the presence of a magnetic field are obtained from the eigenvalues of the tensor $\hat{\mathbf{z}} \times \hat{\mathbf{z}} \times \epsilon^{-1}$ [38]. These indices determine the resonance frequencies of the eigenpolarizations in the resonator (we do not consider magnetostriction here). They are therefore functions of the external magnetic field. Obviously, a small sensitivity of these frequencies on the field is desired. The general solution shows that we can distinguish two cases.

The first case is when in the absence of a magnetic field the medium does exhibit birefringence for the chosen direction of propagation, i.e., $n_x \neq n_y$. The relative change in the eigenindices in the presence of a field is approximately given by

$$\frac{\Delta n_{x,y}}{n_{x,y}} = \pm \frac{(\gamma B_z)^2}{2n_{x,y}^2(n_x^2 - n_y^2)}. \qquad \text{(A2)}$$
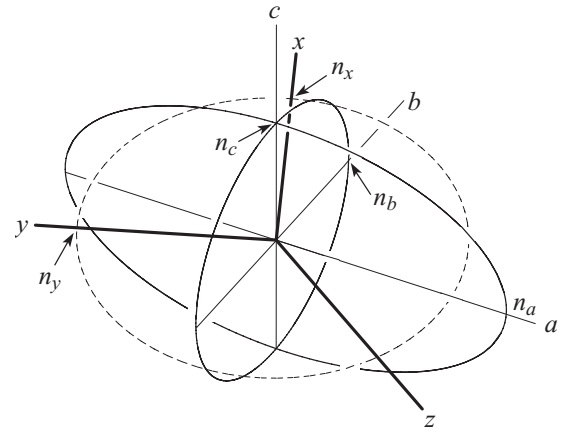

FIG. 4. Geometry considered for magneto-optic effects. The index ellipsoid in the principal axis system (a,b,c) with semiaxis lengths n_a, n_b, n_c (principal indices) is shown. For a given propagation direction z, the intersection of the index ellipsoid with a plane through the origin and normal to z defines an ellipse (dashed line). Its minor and major axes (x, y) are the directions of the eigenpolarizations of the displacement field vector. Their lengths n_x, n_y are the eigenindices.

Contributions from B_x^2 and B_y^2 are neglected since they are smaller. Thus the shifts are quadratic in the magnetic field component in the propagation direction, and the eigenpolarizations remain (for realistic magnetic fields) nearly linear [39].

In a resonator made of such a material, the resonance frequencies in absence of a B field will be well separated, since the static birefringence $n_x - n_y$ will typically cause a sufficient difference in the free spectral ranges, $c/n_x L_{rt}$ and $c/n_y L_{rt}$. If under this condition a laser wave has one of the two eigenpolarizations and is locked to the corresponding eigenmode, the relative frequency shift $\Delta \nu / \nu$ for a nonzero magnetic field is given by the above relative change in the eigenindex $\Delta n / n$. Thus the frequency shift will be quadratic in an applied magnetic field (analogous to a quadratic Zeeman effect), with a typical value $\pm 10^{-20}(B/G)^2$ for $|n_x - n_y| = 0.01$. At the required 10^{-18} level of constancy of n (see Sec. IV), the influence of the magnetic field appears easily controllable.

As a second case we consider absence of birefringence $n_x = n_y = n$, which implies that the propagation direction is along an optic axis. In optically isotropic media this is the case for all propagation directions. The index shift is, to lowest order in the magnetic field components,

$$\frac{\Delta n_{x,y}}{n} = \pm \frac{\gamma B_z}{2n^2}. \qquad \text{(A3)}$$

The eigenpolarizations are circular in this case, and as a consequence linearly polarized light experiences a polarization rotation. This is the commonly known Faraday effect, with the rotatory power given by the Verdet constant $V = \gamma \omega / 2c$.

In a resonator, the eigenfrequencies are polarization degenerate in the absence of a field. This degeneracy is removed when a field is applied, and the eigenpolarizations are

the left and right circular polarizations. When a circularly polarized laser wave is locked to one of these two eigenmodes, its frequency shifts linearly with field (analogous to a linear Zeeman effect), by a relative amount given by Eq. (A3), with a typical magnitude of $10^{-10}B/G$.

This shift is very large even for small magnetic fields if compared to the necessary constancy of n. A reduction of the influence of magnetic field can be achieved by effective shielding and by using linearly polarized light to interrogate the resonator. The error signals generated by the two counterrotating circular polarizations contained in the linearly polarized wave could be added such that a strong common mode rejection of the magnetic field contribution results. While this appears feasible, the first case is more favorable and we are led to conclude that one should preferably use an optically anisotropic crystal and design the resonator such that the resonator mode does not propagate along an optic axis.

APPENDIX B: STRONGLY DISPERSIVE RESONATOR

We consider here the case of a medium with a large difference of the dispersions at the two frequencies ω_1 and ω_2. For an ionic solid, tuning the lower frequency towards the phonon frequencies increases the dispersion, but the absorption will grow exponentially [14], so this situation is not favorable. Instead we consider the deliberate doping of the medium with impurity ions having an electronic transition and tuning one of the two laser frequencies to the vicinity of the impurity resonance. Since we have shown above that the dispersion due to the phonons is small in typical materials, we neglect it altogether.

We can model this situation by a susceptibility $\xi(\omega)$ that contains the atomic contribution ξ_{at} and a term due to a concentration N' of two-level systems of transition energy Ω' and oscillator strength f':

$$\mathrm{Re}\chi'_{el}(\omega) = \frac{N'e^2}{\epsilon_0 m_e}\frac{f'}{\Omega'^2 - \omega^2}. \quad (B1)$$

Now Ω' is an electronic energy, $\Omega' \sim E_R/\hbar$. In this case, $\mathrm{Re}\,\chi'_{el}(\omega)$ obviously does not depend on m_e/m_p. Explicitly,

$$\mathrm{Re}\,\chi'_{el}(\omega) = \frac{F'}{1 - \alpha^{-4}\omega^2/\bar{\omega}'^2}, \quad (B2)$$

with time-independent $\bar{\omega}' = \pi\hat{\Omega}'c/\Lambda$ and dimensionless $F', \hat{\Omega}'$. Relation (8) holds here as well.

The measurement we consider is with ω_1 far off resonance ($\bar{n}_1 = 0$) and with ω_2 close to a harmonic of ω_1 and weakly detuned from the ions' resonance frequency Ω'. This scheme effectively means performing a comparison of the frequency of a cavity with the frequency of an electronic transition, but instead of having separate systems, the comparison is realized in a single system, the doped monolithic cavity. The scheme allows for a sensitive test of $d\alpha/dt$, but not of $d(m_e/m_p)/dt$.

The frequency difference is given, following a calculation similar to Sec. III, by

$$\Delta\omega_f - \Delta\omega_1 = \frac{\bar{n}_2}{1 + \bar{n}_2}\left(\frac{\Delta\alpha}{\alpha} + \frac{\Delta L_{rt}|_e}{L_{rt}}\right)\omega_1$$
$$+ \left(\frac{\Delta n_1|_e}{n_1} - \frac{\Delta n_2|_e/\bar{n}_2}{1 + \bar{n}_2}\right)\omega_1 + \frac{\Delta\omega_{e2}/2}{1 + \bar{n}_2} - \Delta\omega_{e1}. \quad (B3)$$

This expression shows that it is highly favorable to have $\bar{n}_2$ of order 1 or larger. Then the drifts of the indices, $\Delta n_i|_e$, and of the lock errors, $\Delta\omega_{ei}/\omega_1$, need only be reduced to the level of the desired measurement goal, $\Delta\alpha/\alpha$. This means a reduction of the drift levels by a factor of 100 compared to the case of weak dispersion.

The requirement for the lock error of wave 2, $\Delta\omega_{e2}/\omega_1$, must take into account that absorption occurs concomitant with the large dispersion $\bar{n}_2 \simeq 1$ assumed. It is determined by the imaginary part of the susceptibility:

$$\mathrm{Im}\,\chi'_{el}(\omega) = -\frac{N'e^2}{\epsilon_0 m_e}\frac{2\omega\Gamma'f'}{(\Omega'^2 - \omega^2)^2}. \quad (B4)$$

Γ' is the angular frequency FWHM linewidth of the absorption, and the above expressions for χ'_{el}, Eqs. (B1), (B4), hold as long as the detuning from resonance is much larger than the linewidth, $|\Omega' - \omega| \gg \Gamma'$. The power absorption coefficient is $\xi_{el}(\omega) = \omega|\mathrm{Im}\,\chi'_{el}(\omega)|/n(\omega)c$. This results in an increase of the resonator linewidth ω_r (FWHM), which is given by

$$\omega_{r2} = \omega_{r2}^{(0)} + \frac{c\xi_{el}(\omega_2)}{n_2} = \omega_{r2}^{(0)} + \frac{18\bar{n}_2}{(n_2^2 + 2)^2}\Gamma', \quad (B5)$$

where $\omega_{r2}^{(0)}$ is the resonator linewidth at ω_2 in the absence of dopant ions. In the second step, the explicit form of the dispersion $\bar{n}_2$ was used. The lock error will be proportional to the linewidth, $|\Delta\omega_e| \simeq \delta\omega_r$. The requirement that $|\Delta\omega_{e2}/2(1 + \bar{n}_2)|$ be sufficiently less than $\omega_1|\Delta\alpha|/\alpha$ finally leads to two requirements

$$\delta\frac{\omega_{r2}^{(0)}}{2(1 + \bar{n}_2)} \ll \omega_1\frac{|\Delta\alpha|}{\alpha}, \quad \Gamma'\delta \ll \frac{(1 + \bar{n}_2)(n_2^2 + 2)^2}{18\bar{n}_2}\omega_1\frac{|\Delta\alpha|}{\alpha}. \quad (B6)$$

For a measurement goal $|\Delta\alpha|/\alpha < 4 \times 10^{-15}$, the requirements for $\omega_{r1,2}^{(0)}$ can be satisfied if the lock accuracy $\delta = 1 \times 10^{-5}$ can be maintained over the duration of the test (1 yr) and if the resonator linewidth $\omega_{r1,2}^{(0)}/2\pi < 100$ kHz in the absence of impurities, implying loss coefficients below 30 ppm/cm. Such levels have already been achieved (see Sec. V).

Furthermore, the condition on the impurity linewidth yields $\Gamma'/2\pi < 100$ kHz, assuming $\bar{n}_2 = 1$ and no significant

enhancement of n_2 (which is achievable for a given detuning $\Omega' - \omega_2$ by choosing a sufficiently low concentration N'). Homogeneous linewidths of intrashell transitions of many rare-earth impurities in various host crystals are at or below this level at cryogenic temperature [42].

As one of many practical issues one must consider that in a solid the transition frequencies of impurities depend on the lattice spacing, among other factors, and thus on the temperature of the crystal. This gives an additional contribution to $\Delta n_2|_e$ that must be controlled. It should also be mentioned that the narrow intrashell transitions in rare-earth ions are almost forbidden, and the nonzero oscillator strengths f' arise from parity-mixing crystal field effects. A more detailed analysis is therefore required to verify whether f' is indeed independent of α.

In a molecular solid (e.g., solid H_2 [40]) or a solid doped with molecules, strong dispersion may also occur. The mo-lecular contribution to the real part of the susceptibility is as in Eq. (7), where the Ω_i are fundamental and overtone vibrational frequencies of the molecules, neglecting the influence of the phonon bands. The imaginary part of the susceptibility corresponding to Eq. (7) is given by an expression analogous to Eq. (B4), but with m_e and Ω' replaced by a constant time m_p and one of the molecular vibrational frequencies Ω_i, respectively.

The advantage of using strong dispersion in a molecular solid instead of in a doped solid with electronic transitions is that the possibility of testing for both $d\alpha/dt$ and $dm_e/m_p/dt$ is retained: in Eq. (B3), $-(m_p/2m_e)\Delta(m_e/m_p)$ is to be added to $\Delta\alpha/\alpha$.

In conclusion, for strong dispersion, the index drift, lock drift, and crystal loss requirements are much less stringent in comparison to weak dispersion. The length relaxation requirement is equally strong [41–43].

---

[1] C.M. Will, *Theory and Experiment in Gravitational Physics* (Cambridge University Press, Cambridge, England, 1993), p. 31.

[2] For introductions, see T. Damour, in Proceedings of the 34th Rencontres de Moriond, "Gravitational Waves and Experimental Gravity," 1999; J.D. Barrow, in *Proceedings of Erice Summer School*, *Primordial Cosmology,* edited by A. Sanchez and A. Zichichi (World Scientific, Singapore, 1998), pp. 269–305, gr-qc/9711084.

[3] T. Damour and F. Dyson, Nucl. Phys. **B480**, 37 (1996).

[4] J.K. Webb *et al.*, Phys. Rev. Lett. **82**, 884 (1999).

[5] L.L. Cowie and A. Songaila, Astrophys. J. **453**, 596 (1995).

[6] E.W. Kolb, M.J. Perry, and T.P. Walker, Phys. Rev. D **33**, 869 (1986).

[7] C.L. Carilli, K.M. Mentem, J.T. Stocke, E. Perlman, R. Vermeulen, F. Briggs, A.G. de Bruyn, J. Conway, and C.P. Moore, Phys. Rev. Lett. **85**, 5511 (2000).

[8] A.Y. Potekhin, A.V. Ivanchik, D.A. Varshalovich, K.M. Lanzetta, J.A. Baldwin, G.M. Williger, and R.F. Carswell, Astrophys. J. **505**, 523 (1998).

[9] J.D. Prestage, R.L. Tjoelker, and L. Maleki, Phys. Rev. Lett. **74**, 3511 (1995).

[10] A. Godone, C. Novero, P. Tavella, and K. Rahimullah, Phys. Rev. Lett. **71**, 2364 (1993).

[11] J.P. Turneaure, C.M. Will, B.F. Farrel, E.M. Mattison, and R.F.C. Vessot, Phys. Rev. D **27**, 1705 (1983).

[12] The α dependence of the dielectric constant of monolithic microwave oscillators has also been considered by Langham and Gallop, with a different aim, however: C.D. Langham and J.C. Gallop, IEEE Trans. Instrum. Meas. **46**, 130 (1997).

[13] W.K.H. Panofsky and M. Phillips, *Classical Electricity and Magnetism* (Addison-Wesley, Reading, MA, 1962).

[14] S.S. Mitra, in *Handbook of Optical Constants of Solids*, edited by E.D. Palik (Academic, New York, 1985), Chap. 11; M.E. Thomas, in *Handbook of Optical Constants of Solids II*, edited by E.D. Palik (Academic, New York, 1991), Chap. 8.

[15] M. Hass, Opt. Eng. (Bellingham) **17**, 525 (1978)

[16] D. Blair, F. Cleva, and C.N. Man, Opt. Mater. **8**, 233 (1997).

[17] N. Ashcroft and D. Mermin, *Solid-State Physics* (College Editions, Fort Worth, TX, 1976).

[18] P. Sisterna and H. Vucetich, Phys. Rev. D **41**, 1034 (1990).

[19] M.J. Weber, *CRC Handbook of Laser Science and Technology* (CRC, Baton Rouge, FL, 1986).

[20] *Handbook of Optical Constants of Solids II* [14], p. 815.

[21] *Handbook of Optical Constants of Solids II* [14], p. 899.

[22] *Handbook of Optical Constants of Solids III*, edited by E.D. Palik (Academic, New York, 1998), p. 653.

[23] *Handbook of Optical Constants of Solids* [14], p. 719.

[24] W.L. Wolfe and G.J. Zissis, *The Infrared Handbook* (Superintendent of Documents, Washington, DC, 1978).

[25] R. Storz, C. Braxmaier, K. Jäck, O. Pradl, and S. Schiller, Opt. Lett. **23**, 1031 (1998).

[26] It is also conceivable that an appropriately made monolithic resonator can be operated at a temperature or with a frequency pair ω_1, ω_2 such that the temperature dependence of the contributions from $\Delta L_{rt}|_e$ and $\Delta n_i|_e$ vanishes: i.e.,

$$\frac{1}{1+\bar{n}_1}\left(L_{rt}^{-1}\frac{dL_{rt}}{dT} + n_1^{-1}\frac{dn_1}{dT}\right) - \frac{1}{1+\bar{n}_2}\left(L_{rt}^{-1}\frac{dL_{rt}}{dT} + n_2^{-1}\frac{dn_2}{dT}\right) = 0.$$

Such a particular operating point can be searched for experimentally. In microwave resonators compensation of the temperature dependence of the absolute frequency (not of the difference of two frequencies as above) has been demonstrated both by doping the dielectric with ions and making a composite resonator formed by parts of different materials. See M.E. Tobar, J. Krupka, J.G. Hartnett, E.N. Ivanov, and R.A. Woode, IEEE Trans. Ultrason. Ferroelectr. Freq. Control **45**, 830 (1998); J.G. Hartnett, M.E. Tobar, A.G. Mann, E.N. Ivanov, J. Krupka, and R. Geyer, *ibid.* **46**, 993 (1999).

[27] Monolithic optical resonators have been used at room temperature for quantum-optical studies starting about a decade ago. These were fabricated from nonlinear-optical crystals such as lithium niobate and potassium niobate. Such crystals typically have substantial loss, and moreover are electro-optic, so they are not suited for the present application. Monolithic resonators made of fused silica were first studied a decade ago [28].

This material is of interest due to the extremely low loss exhibited by ultrapure fused silica. With a 7.5×7.5 mm square monolithic fused silica ring resonator based on total internal reflection (fabricated by REO, Boulder, CO) linewidths of 190 kHz at impedance match at a wavelength of 1064 nm were obtained in our group [29]. This corresponds to a *total* (absorption plus scatter) loss coefficient $\xi = 3$ ppm/cm. Pipino [30] recently reported on a similar fused silica resonator with a loss for 580 nm light, equivalent to a 240-kHz linewidth at impedance match. In early works on cryogenic optical resonators, a quartz monolithic optical resonator has been operated at liquid helium temperature [31]. This device, however, possessed a dielectric coating of relatively high transmission and thus exhibited a large linewidth.

[28] S. Schiller, I. Yu, M.M. Fejer, and R.L. Byer, Opt. Lett. **17**, 378 (1992); S. Schiller, A. Sizmann, M.M. Fejer, and R.L. Byer, U.S. Patent No. 5,227,911.

[29] M. Bader, Diploma thesis, Universität Konstanz, 1995.

[30] A.C.R. Pipino, Phys. Rev. Lett. **83**, 3093 (1999).

[31] S. Schiller, S. Seel, R. Storz, and J. Mlynek, Proc. SPIE **2378**, 138 (1995).

[32] J.P. Roger, F. Charbonnier, D. Fournier, and A.C. Boccara, in *Photoacoustic and Photothermal Phenomena II—Proceedings of the 6th International Topical Meeting*, edited by B. Royce and J. Murphy [Springer Ser. Opt. Sci. **62**, 316 (1990)].

[33] See, e.g., B.D. Evans, J. Appl. Phys. **70**, 3995 (1991).

[34] M.E. Innocenzi, R.T. Swimm, M. Bass, R.H. French, A.B. Villaverde, and M.R. Kokta, J. Appl. Phys. **67**, 7542 (1990).

[35] S. Seel, R. Storz, G. Ruoso, S. Schiller, and J. Mlynek, in *Proceedings of the Fifth Symposium on Frequency Standards and Metrology*, edited by J. Berquist (World Scientific, Singapore, 1996), pp. 347–352.

[36] Y.S. Touloukian, R.K. Kirby, R.E. Taylor, and T.Y.R. Kee, *Thermophysical Properties of Matter* (IFI/Plenum, New York, 1977), Vol. 13.

[37] S.A. Diddams, D.J. Jones, J. Ye, S.T. Cundiff, J.L. Hall, J.K. Ranka, R.S. Windeler, R. Holzwarth, T. Udem, and T.W. Hänsch, Phys. Rev. Lett. **84**, 5102 (2000).

[38] A. Yariv and P. Yeh, *Optical Waves in Crystals* (Wiley, New York, 1984), Chap. 4.

[39] See also W. Schütz, in *Handbuch der Experimentalphysik* (Akademische Verlagsgesellschaft, Leipzig, 1936), Vol. XVI-1.

[40] J. Van Kranendonk, *Solid Hydrogen* (Plenum, New York, 1983).

[41] J.A. Harrington, D.A. Gregory, and W.F. Otto, Appl. Opt. **15**, 1953 (1976); *Optical Properties of Highly Transparent Solids*, edited by S.S. Mitra and B. Bendow (Plenum, New York, 1975).

[42] R.W. Equall, Y. Sun, R.L. Cone, and R.M. Macfarlane, Phys. Rev. Lett. **72**, 2179 (1994).

[43] C. Braxmaier, O. Pradl, B. Eiermann, A. Peters, J. Mlynek, and S. Schiller, in Proceedings of the Conference on Precision Electromagnetic Measurements, 2000 (IEEE Instrumentation and Measurement Society, 2000).